

State-space of deterministic system

August 17, 2023

Arman Behrad

1 Introduction

Fuster (Fuster, 1995) demonstrated that neurons in the prefrontal or temporal cortex continue to exhibit firing activity even after the disappearance of the specific stimulus associated with each neuron, as observed in delayed response tasks.

Building upon Fuster's findings, Wilson (Wilson, 1999) proposed a simplified system composed of two mutually excitatory neurons, whose spike rates are characterized by the Naka-Rushton function. In this model, the neurons are assumed to possess identical properties and connection strengths, leading to the following set of equations:

$$\begin{aligned}\tau \frac{dE_1}{dt} &= -E_1 + \phi[wE_1 - E_2 - 0.5] \\ \tau \frac{dE_2}{dt} &= -E_2 + \phi[E_1 - E_2 - 0.5] \\ \phi(x) &= \frac{x^2}{\kappa^2 + x^2}\end{aligned}$$

Where $\tau = 10$ and $\kappa = 0.75$. The depiction of our system is as follows:

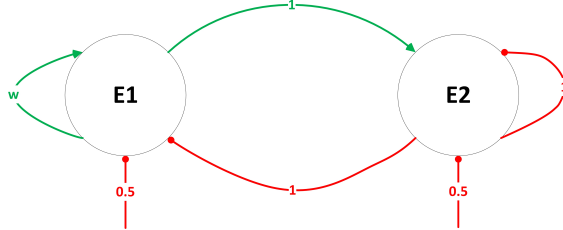


Figure 1: Depiction of the System. In this system, E_1 states for Excitatory population and E_2 for Inhibitory.

In the current study, our objective is to comprehensively explore the behavior of this neural system. Specifically, we aim to elucidate the system's steady states, which are critical points of neural activity that play a significant role in understanding the system's overall dynamics. Furthermore, we seek to investigate the influence of several key parameters, notably the synaptic weight (w) governing the strength of connections between the populations, as well as the initial positions of neurons within each population.

This investigation holds promise for advancing our understanding of neural network dynamics and may contribute to unraveling the underlying principles governing neural information processing. By unraveling how different system parameters impact the behavior of the neural network, we can gain valuable insights into its functionality and potentially uncover novel avenues for neural network engineering and design.

The subsequent sections of this paper are organized as follows: In Section 2, we present the mathematical framework underpinning the interaction between the excitatory and inhibitory neuron populations. Section 3 delves into the analysis of steady states and their stability. The simulation methodology and results are outlined in Section 4. We subsequently engage in a discussion of our findings and their implications in Section 5, while also suggesting potential directions for future research.

2 Time Evolution of System

To explore the dynamics of the neural system, we initiated simulations of cellular activities over time, considering an initial position of $X_0 = [0, 0]$ and various values of synaptic weight (w , where $2 < w < 4$). The activity of the neuron populations was simulated using an iterative integration approach, as described by the following equation:

$$E_{i+1} = E_i + (E_{ss} - E_i) \left(1 - \exp \left(-\frac{dt}{\tau} \right) \right)$$

Here, E_{ss} represents the fixed point activity for each population, $dt = 0.0001$, and $\tau = 0.1$.

Figure 2 illustrates the activity of each population as a function of time. Initially starting from $[0,0]$, both populations exhibit an increase in response amplitude until reaching a steady state, thereafter maintaining a constant activity level. Notably, the excitatory population consistently displays higher amplitude activity compared to the inhibitory population. The specific values of these steady states for each population are influenced by the parameter w . Subsequent analysis seeks to determine the fixed points of the system by identifying the isoclines through the equations:

$$\begin{aligned} E_1 &= \phi[wE_1 - E_2 - 0.5] \\ E_2 &= \phi[E_1 - E_2 - 0.5] \end{aligned}$$

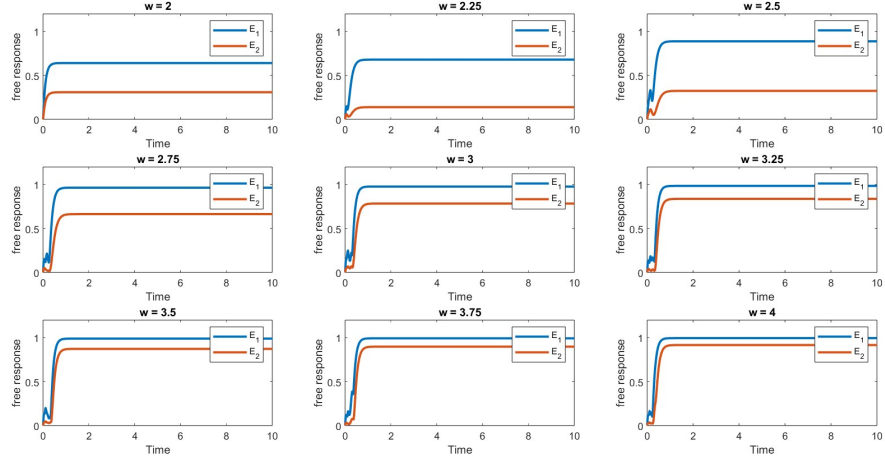


Figure 2: Activity of each population over time. Initial states for both populations are $[0,0]$. Following an initial response amplitude increase, both populations converge to steady states with distinct activity levels. Notably, the steady state values vary for different w values.

Figure 3 provides insight into the isoclines for both populations. The intersections of these lines determine the fixed points of the system, reflecting the equilibrium states that the system tends to attain.

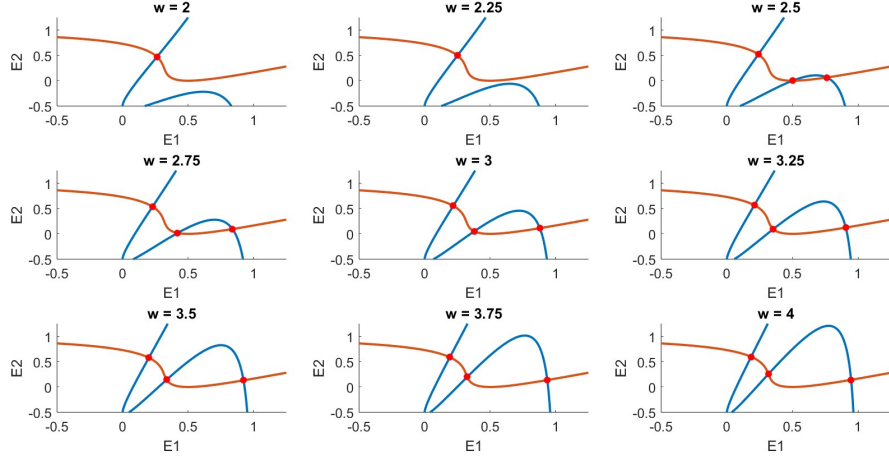


Figure 3: Isoclines for the two populations. The points of intersection (denoted by dots) reveal the fixed points of the system.

This analysis sheds light on the intricate relationship between the system's parameters, such as synaptic weight and initial conditions, and the resulting neural dynamics. The subsequent sections delve deeper into the interpretation and implications of these findings.

3 Steady State Analysis

The behavior of the system is notably influenced by different values of w , as depicted in Figure 3. Steady states manifest in various numbers and positions with respect to w . For instance, when $w = 2$, the system exhibits only one steady state located at $E_1 = 0.2625$ and $E_2 = 0.4727$. Conversely, for $w = 4$, there are three steady states positioned at: $E_1 = 0.1847, E_2 = 0.5962$; $E_1 = 0.3162, E_2 = 0.2548$; and $E_1 = 0.9461, E_2 = 0.1415$.

By employing isoclines and fixed points, distinct regions of behavior within the system can be defined. However, the nature of this behavior, such as stability, instability, or saddle points, remains ambiguous. To gain a clearer understanding, we proceed to introduce the concept of the 'Flow Field' to our analysis.

4 Flow Field

In order to visualize the system's dynamics, we introduced auxiliary variables as follows:

$$F_1 = \tau \frac{dE_1}{dt}$$

$$F_2 = \tau \frac{dE_2}{dt}$$

We computed the dynamic vector (F_1, F_2) at selected positions and juxtaposed the resulting flow field with the trajectories obtained from the time evolution of the system with diverse initial conditions:

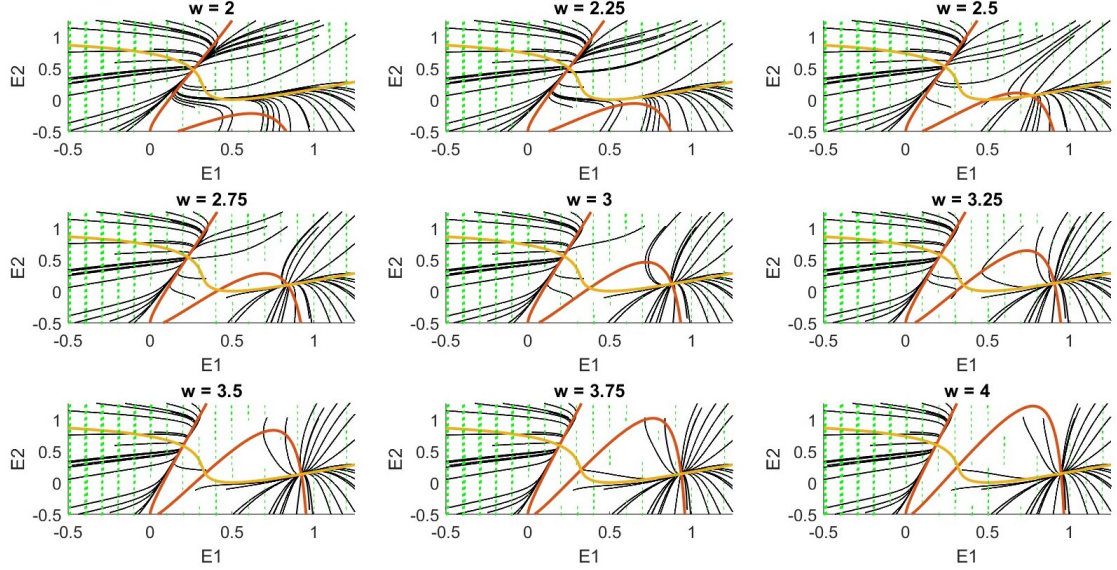


Figure 4: Trajectory of the system, along with the flow field and isolines. Trajectories, represented by black lines, align consistently with the flow field's green arrows and the previously determined isolines and fixed points, confirming the accuracy of the analysis.

Figure 4 convincingly demonstrates the alignment between the trajectories of the time-evolving system (black lines), the flow field (green arrows), and the calculated isolines and fixed points. This congruence provides empirical validation for the theoretical analysis conducted thus far. For deeper insights, we narrow our focus to $w = 4$, offering a detailed exploration of its behavior.

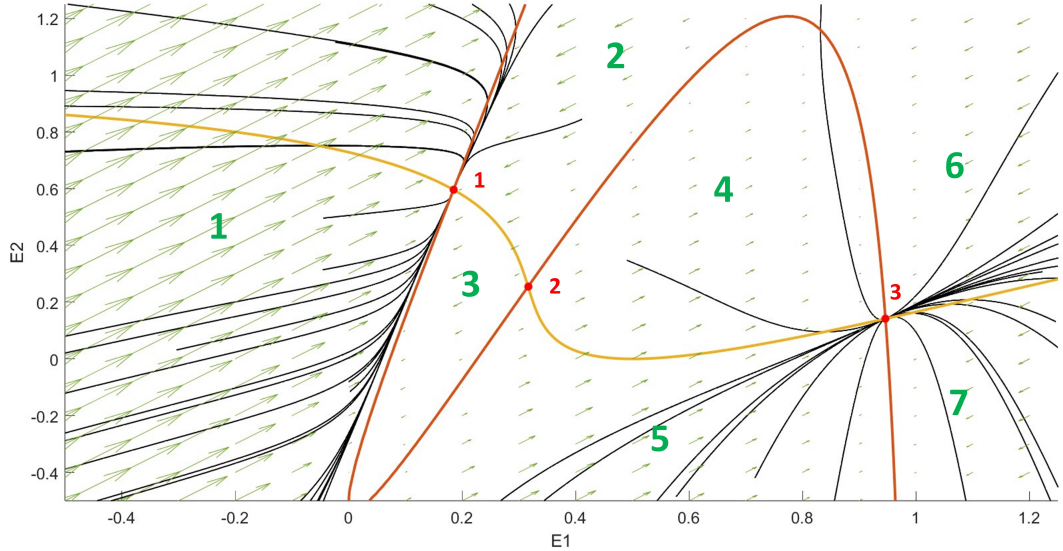


Figure 5: System trajectory, flow field, and isoclines for $w = 4$. The graph is divided into regions, each marked with a green number, and various steady states are denoted by red numbers.

Figure 5 illustrates distinctive regions of activity for the system with $w = 4$. Within region 1 (marked by the green number), the flow field indicates trajectories converging toward steady state number 1 (highlighted by the red number). Trajectories originating within this region consistently lead to the attainment of fixed point number 1. Notably, fixed point number 2 is unstable, while fixed point number 3 is stable.

To further explore the influence of system constants, particularly w , we introduce the Bifurcation Diagram as a valuable tool.

5 Bifurcation Diagram

A Bifurcation Diagram provides insights into the system's asymptotic behaviors, such as fixed points, periodic orbits, or chaotic attractors, as a function of a designated bifurcation parameter (May, 1975). In our context, we present the steady states of the excitatory population E_1 as a function of the synaptic weight w :

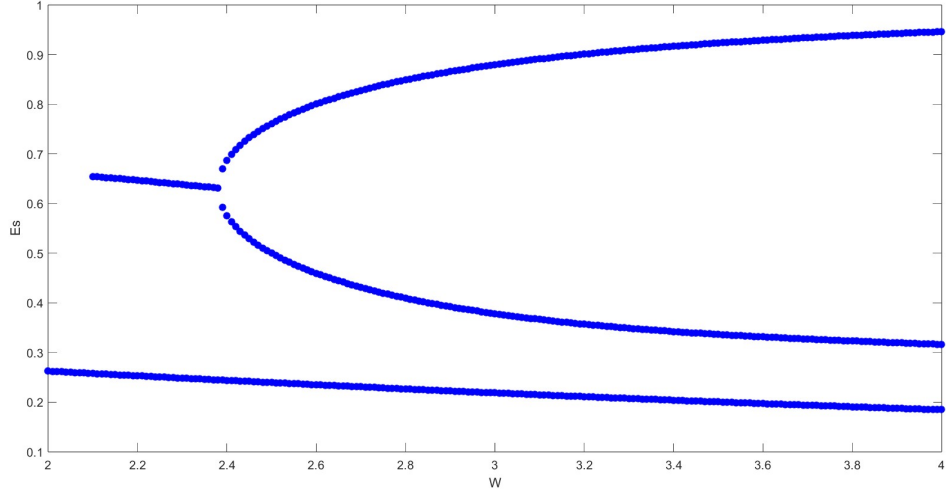


Figure 6: Bifurcation Diagram illustrating the steady states of the excitatory population E_1 as a function of the synaptic weight w . Distinct behaviors emerge for different ranges of w .

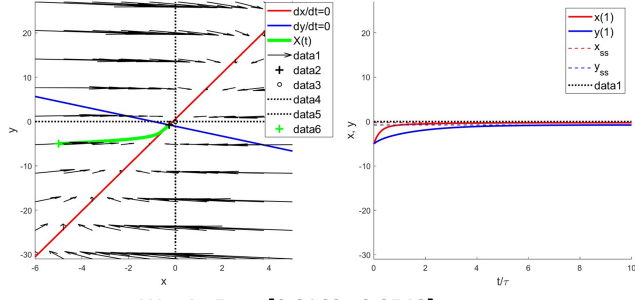
6 Jacobian Matrix

The Jacobian matrix, an essential tool in analyzing dynamical systems, provides valuable insights into the system's behavior. Computed for our system, the Jacobian matrix is defined as follows:

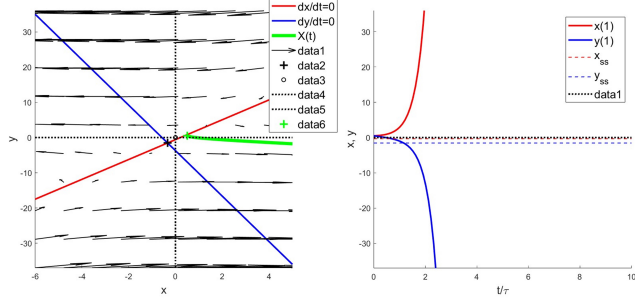
$$J = \begin{bmatrix} -\frac{8(4x-y-0.5)^3}{((4x-y-0.5)^2+0.5625)^2} + \frac{8(4x-y-0.5)}{(4x-y-0.5)^2+0.5625} - 1 & \frac{2(4x-y-0.5)^3}{((4x-y-0.5)^2+0.5625)^2} - \frac{8(4x-y-0.5)}{(4x-y-0.5)^2+0.5625} \\ \frac{2(4x-y-0.5)}{(4x-y-0.5)^2+0.5625} - \frac{2(4x-y-0.5)^3}{((4x-y-0.5)^2+0.5625)^2} & \frac{2(4x-y-0.5)^3}{((4x-y-0.5)^2+0.5625)^2} - \frac{2(4x-y-0.5)}{(x-y-0.5)^2+0.5625} - 1 \end{bmatrix}$$

As an illustration, we solved the Jacobian for $w = 4$ and its three identical steady states. The numerical results were then fed into the function **LinearOrder2**. Subsequently, we compared the flow field and nullclines of the Jacobian matrix with the trajectories of the system's time evolution:

W = 4, Ess = [0.1847 , 0.5962]



W = 4, Ess = [0.3162 , 0.2548]



W = 4, Ess = [0.9461 , 0.1415]

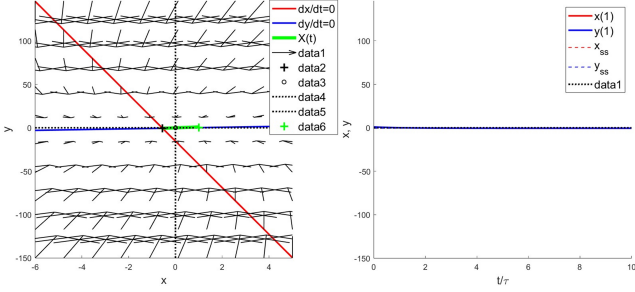


Figure 7: Flow field and nullclines of the Jacobian matrix for $w = 4$. Trajectories and fixed points closely align with the theoretical predictions, affirming the stability analysis conducted using the Jacobian matrix.

The analysis of the Jacobian matrix, depicted in Figure 7, confirms that the theoretical stability predictions align remarkably well with the actual trajectories of the system's time evolution. For instance, the eigenvalues for the first steady state ($E_1 = 0.1847, E_2 = 0.5962$) are $\lambda_1 = -4.5732$ and $\lambda_2 = -0.5895$, indicating a stable point. Similarly, for the second steady state ($E_1 = 0.3162, E_2 = 0$)

References

- Fuster, J. M. (1995). Memory and planning: Two temporal perspectives of frontal lobe function.
- May, R. M. (1975). Biological populations obeying difference equations: stable points, stable cycles, and chaos. *Journal of Theoretical Biology*, 51(2):511–524.
- Wilson, H. R. (1999). Spikes, decisions, and actions: Dynamical foundations of neuroscience.